

Computer Simulation of Induction Heating Process of Hot Rolled Slab

Cheng Xiaoming, Xu Zhe, and He Bishi

Automation College, Hangzhou Dianzi University, Hangzhou, Zhejiang, 310018, China

Email: 1477097927@qq.com, {xuzhe, hebishi}@hdu.edu.cn

Abstract—In this paper, the three-dimensional dynamic model of slab induction heating and soaking process is established by finite element method. Two different width to thickness ratio slabs are simulated at constant speed through the heating process of the inductor and the subsequent soaking process. Then the temperature field diagram of induction heating and soaking at different moments was obtained, and the regularity and characteristics of temperature change during induction heating were analyzed. Finally the following conclusions are obtained, (1)the greater the width to thickness ratio of the slab, the greater the temperature difference after induction heating, (2)the reasonable setting of the soaking period will help the slab temperature tend to be uniform, and (3)the addition of the insulation cover can effectively delay the slab cooling.

Index Terms—slab induction heating, finite element method, numerical simulation

I. INTRODUCTION

A. Slab Induction Heating Background

Slab electromagnetic induction heating is the use of electromagnetic induction in the surface area of the slab to produce eddy current, compared to the traditional gas heating, It have no pollution, high efficiency, precise control, ready to use and other characteristics, Electromagnetic induction heating is gradually applied in the iron and steel hot rolling production line.

Induction heating process involves electric field, magnetic field and temperature field, the traditional engineering calculation method is too simplistic, the calculation results and the actual deviation is large, we cannot get the internal temperature of slab. With the development of computer technology, modern numerical simulation technology not only reduces the calculation time greatly, but also improves the accuracy of the calculation. Finite element method is one of the commonly used numerical simulation [1], [2].

Many scholars have made extensive research on the numerical simulation of induction heating. Most scholars have studied the induction heating of billet and cylinder blank [3]-[6], but it also lacks in-depth study on slab. As slabs in today's industrial production has an expanding market. comparing to the billet and cylindrical billet, slab has a large aspect ratio, heat dissipation surface area, the

induction heating put forward higher technical requirements.

This paper is based on the previous project [7], [8]. A study was conducted on two kinds of slabs with different aspect ratios. The dynamic heating and soaking process were investigated by analyzing the 3D model of slab induction heating.

II. ANSYS FINITE ELEMENT METHOD SIMULATION

A. Basic Assumptions and Simplification

In this paper, two kinds of slabs with different width to thickness ratio A (720mm * 120mm * 6000mm) and B (1440mm * 120mm * 6000mm) are selected. The length is 6m and the aspect ratio is 6: 1, 12: 1. Sensor coil 20 turns, length 1m, design power 2500kw, slab induction heating before the initial temperature of 800 °C, slab roller drive speed 5m / min.

In order to reduce the amount of finite element calculations, the simplification and assumptions of the induction thermal physical process model are as follows:

Related to electromagnetic fields

1) The induction heating device is powered by the 1000Hz intermediate frequency power supply, ignoring the displacement current (quasi-static condition).

2) When the sinusoidal alternating current is introduced into the induction coil, the alternating electromagnetic field generated by the induction coil is the dynamic electromagnetic field, and the mathematical model of the eddy current field is sinusoidal steady-state problem.

3) Assuming that the initial temperature of the slab before induction heating is uniform at 800 °C, above the Curie point of 780 °C, its relative permeability is equal to 1.

4) In calculating the eddy current distribution in the slab surface area at a certain time, the influence of the generated dynamic electromotive force on the slab is neglected.

5) Slab material isotropic, so the sample can be 1/4 modeling.

About the temperature field

1) The actual situation in the slab from the roller into the sensor before the overall temperature is very uneven, this simulation assumes that the slab into the sensor before the overall temperature distribution uniformity of 800 °C.

2) During the process of slab, the influence of the roller on the slab temperature field is very small, ignoring the influence of the roller on the heat transfer on the lower surface of the slab [9].

3) In the case of high temperature, the metal is mainly distributed mainly radiant heat. The convective heat dissipation is only 2-10% of the total heat dissipation part. Therefore, it can be neglected in general to correct the convective heat caused by the deviation [10].

4) Ignoring the effect of iron oxide on the heat transfer on the slab surface.

B. Slab Movement

The movement of billet in this paper is the use of load movement to achieve the relative movement of the coil and billet as shown in Fig. 1. The current path of the coil is pre-divided into the grid. At the moment, the first pair of arrows contains the current load in the coil area, and the current load is loaded in the coil region included in the second pair of arrows. The distance of the load movement is exactly the distance from the billet. The numbers of segments are smaller, the accuracy of the calculation are smaller, the relative calculation time are longer. The number of segments can be obtained by using the trial and error method. The simulation results are approximated with the pre-analysis results or the actual data. An appropriate value is obtained between the precision and the calculation time. The number of segments set by this method is 25. Here the model assumes the following assumptions:

- 1). Do not take into account the gap between the turns of the coil;
- 2). Regardless of the coil motion path on the coil material and air resistivity and permeability of the different effects;

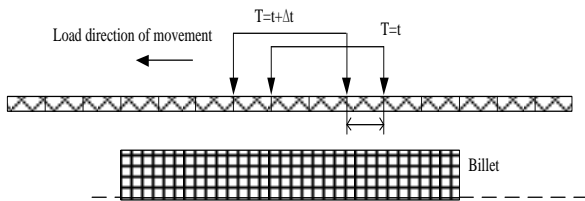


Figure 1. Billet motion diagram

C. Boundary Conditions

Magnetic analysis: It is very weak almost 0 closely to the slab from the location of the magnetic flux intensity so the need to set its magnetic potential 0, far field and the symmetry of the magnetic potential is set to 0, usually we will board The voltage at one end of the blank or coil is set to 0, the other end of the coupling VOLT degree of freedom, and then apply a load to each of the slabs to excite the electromagnetic field.

Thermal analysis: for coil and air, the temperature field analysis of its unit type is set to NULL, only consider the thermal analysis of slab, the ambient temperature is set to 25 °C, only with the air contact with the outer surface of the slab For thermal radiation exchange, the general value of 0.68.

D. Multi-Physical Field Analysis of Induction Heating

Multi-physics fields are also commonly referred to as coupling fields, and their coupling methods are generally divided into direct coupling and load transfer coupling. The multi-physics field in the induction heating of the billet is the coupling between the electromagnetic field and the temperature field, and not only the electromagnetic field can be applied to the temperature field, but also the temperature field can react to the electromagnetic field and interact with each other. Therefore, during the induction heating process of the coupling phenomenon is often not accurately described. Fig. 2 shows the experimental flow chart of billet finite element simulation.

- 1) Establish the finite element model in the induction heating process.
- 2) Give the billet, air and coil the unit attribute number, and set the physical attributes.
- 3) Create an electromagnetic field analysis file emag, temperature field analysis file thermal and coupling load file hgen.rst.
- 4) Reasonable grid division of billets, respectively, to create a different physical environment for the next step of the electromagnetic field and temperature field analysis, and were written into the emag file and thermal file.
- 5) In the electromagnetic field analysis, read the file emag for electromagnetic field analysis, obtained the coupling load, and deposited into the hgen.rst file.
- 6) In the temperature field analysis, read the load in the hgen.rst file obtained in the previous step plus the load read from the thermal file, and accumulate the solution to obtain the temperature field distribution of the current environment.
- 7) If the heating time has not yet reached or reaches the target temperature, the billet temperature changes affect the material properties, so the next round of electromagnetic field solution.

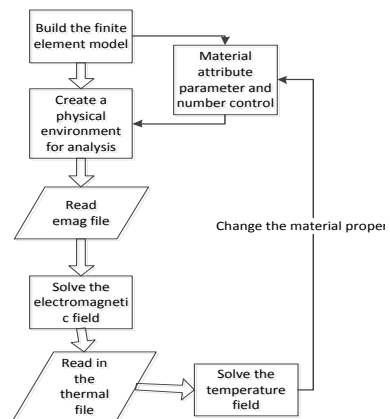


Figure 2. Electromagnetic induction heating experiment flow chart

E. Slab Temperature Field Cloud

In view of the slab length 6m, transmission speed 5m / min, induction coil length of 1 meter, the induction heating time is 80.64s, another soaking time is 30s, the total length of 110.64s. After simulation, It is shown in

Fig. 3a, Fig. 3b that two kinds of slab induction heating at $t_1 = 80.64s$ time temperature field cloud where the slab is at the end of the sensor position. It is shown in Fig. 4a, Fig. 4b that two kinds of slab induction are hot end $t_2 = 110.64s$ time temperature field cloud. 2 slab heating end time $t_1 = 80.64s$ temperature value as shown in Table I, the soaking end time $t_2 = 110.64s$ temperature value as shown in Table II.

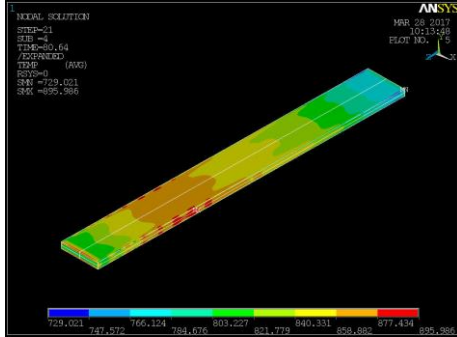


Figure 3.a $t_1 = 80.64s$, slab A

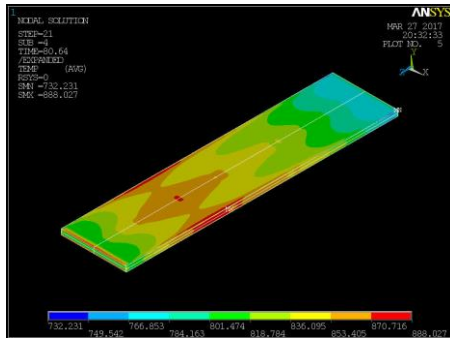


Figure 3.b $t_1 = 80.64s$, slab B

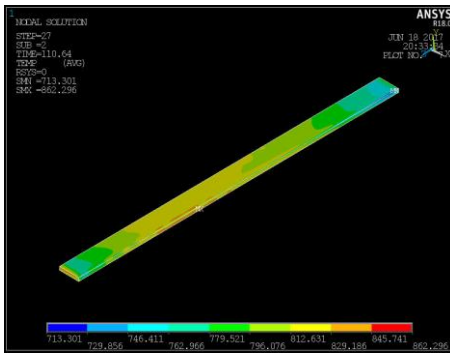


Figure 4.a $t_2 = 110.64s$, slab A

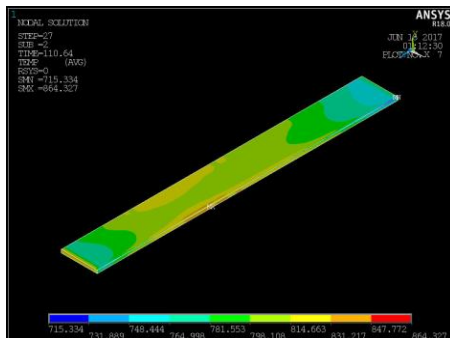


Figure 4.b $t_2 = 110.64s$, slab B

TABLE I. SLAB $t_1 = 80.64s$ THE TEMPERATURE AT THE END OF THE HEATING

| Slabs | Maximum temperature | Minimum temperature | Temperature difference |
|-------|---------------------|---------------------|------------------------|
| A | 895 °C | 729 °C | 166 °C |
| B | 888 °C | 732 °C | 156 °C |

TABLE II. SLAB $t_2 = 110.64s$ THE TEMPERATURE AT THE END OF THE SOAKING TIME

| Slabs | Maximum temperature | Minimum temperature | Temperature difference |
|-------|---------------------|---------------------|------------------------|
| A | 862.3 °C | 713.3 °C | 149.0 °C |
| B | 864.3 °C | 715.3 °C | 149.0 °C |

Analysis: $t_1 = 80.64s$, At the end of the heating, There is small difference in the maximum temperature, minimum temperature, but the aspect ratio of the slab is larger, the temperature distribution on the upper surface of the slab is more complicated. $t_2 = 110.64s$ At the end of the soaking time, There is small difference in the maximum temperature, minimum temperature, but the temperature of the upper surface is still polymorphic. 2 kinds of slab through the soaking process, the temperature difference is further reduced, in the slab hot rolling process, a reasonable set of soaking links can make the slab temperature further uniform.

F. S-S' Section MN Path Temperature Condition

In order to study the cross-section of slab heating and soaking, we take the longitudinal section of the slab as the object of study, marking as S-S' section. because of the symmetry of the slab, we take a quarter of the cross Research, cross-section position and cross-section key points shown in Fig. 5. Where only the temperature in the middle of the upper surface to the corner path MN and the side surface to the corner path PN is shown here.

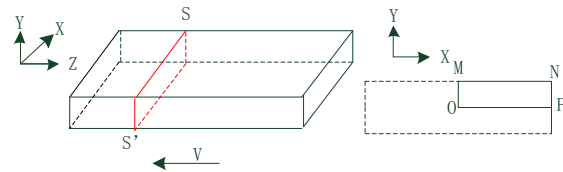


Figure 5. Cross section of slab

As shown in Fig. 6a, Fig. 6b, the temperature distribution curve of the MN path, the bright blue curve, the purple curve, the red curve and the light blue curve of the two slabs S-S' are shown as $t = 0.384s, 38.4s, 57.6s, 80.64s$ MN path temperature distribution, the corresponding slab position is the first side of the slab head into the sensor, slab filled with sensors, slab tail just out of the sensor. As shown in Fig. 7a, Fig. 7b, the temperature distribution curve of the MN path, the bright blue curve, the purple curve, the red curve and the light blue curve of the two slabs S-S' are shown as $t = 0.384s, 38.4s, 57.6s, 80.64s$ MN path temperature distribution. Here, the heating time $t_3 = 38.4s$ as the study time point, two kinds of slab MN path temperature distribution in Table III. Taking the soaking time $t_4 = 110.64s$ as the study time point, two kinds of slab MN path temperature distribution as shown in Table IV.

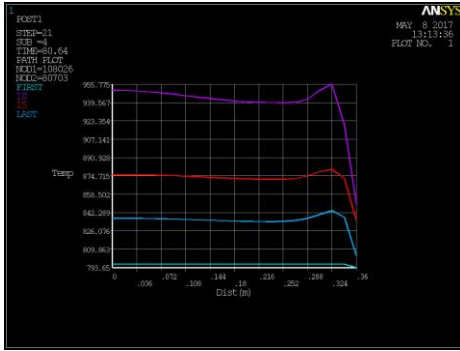


Figure 6.a t3 = 38.4s, slab A

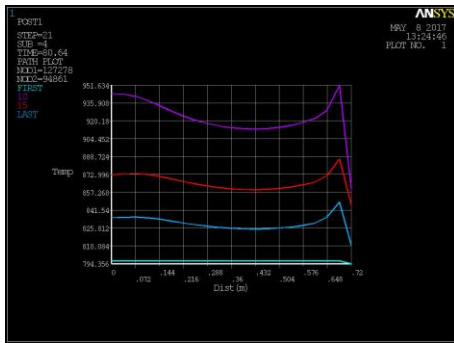


Figure 6.b t3 = 38.4s, slab B

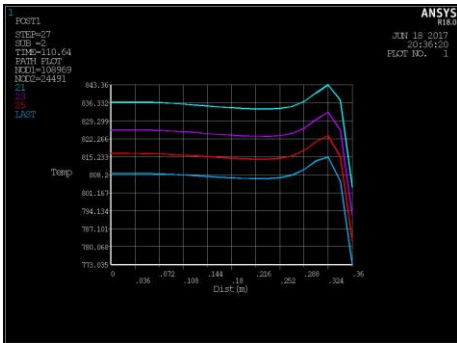


Figure 7.a t4 = 110.64s, slab A

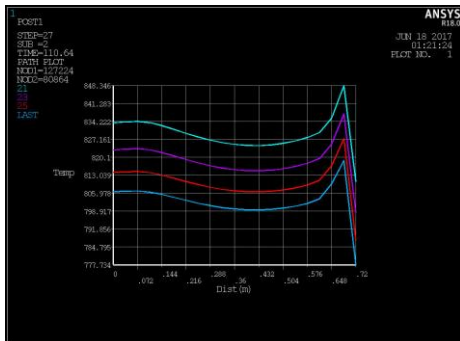


Figure 7.b t4 = 110.64s, slab B

TABLE III. t3 = 38.4s SLAB PATH MN TEMPERATURE COMPARISON

| Slabs | Temperature fluctuation range | Near the corner area temperature peak | Corner zone temperature value |
|-------|-------------------------------|---------------------------------------|-------------------------------|
| A | 10.5 °C | 955.7 °C | 850.3 °C |
| B | 31.3 °C | 951.6 °C | 860.5 °C |

Analysis: In the slab induction heating, $t_3 = 38.4s$, the two slabs are close to the corners the domain has the highest temperature and the corners have the lowest temperature. It is shown that the magnetic field near the corner region is the strongest in the induction heating process, the vortex thermal effect is the strongest, the magnetic field in the corner area is the weakest, the eddy heat effect is the weakest, and the temperature in the middle region is stable. As the thickness ratio of the slab increases, the greater the temperature fluctuation range on the MN path, the more uneven the temperature distribution. So should focus on the slab corner of the heat.

TABLE IV. COMPARISON OF THE TEMPERATURE OF THE SLAB PATH MN IN THE SOAKING STAGE

| Slabs | Slab is hot before $t_3 = 80.64s$ | | | After slabs are hot, $t_4 = 110.64s$ | | |
|-------|-----------------------------------|-------------|-------------------------------|--------------------------------------|-------------|-------------------------------|
| | Near the corner area | Corner area | Temperature fluctuation range | Near the corner area | Corner area | Temperature fluctuation range |
| A | 843.4 °C | 803.0 °C | 3 °C | 815.2 °C | 773.0 °C | 2 °C |
| B | 848.3 °C | 810.0 °C | 9.2 °C | 815.0 °C | 777.0 °C | 7.0 °C |

Analysis: 2 kinds of slab in the soaking after the MN path temperature fluctuations are further reduced, so the reasonable set of soaking links can make the slab temperature further uniform. The greater the thickness ratio of the slab, the greater the temperature fluctuation range at the same time. The maximum temperature changes of the two slabs were 28.2 °C and 33.3 °C, the minimum temperature of the corners was 30.0 °C and 33.0 °C. The greater the thickness ratio of the slab, the faster the maximum temperature drop near the corner area, and the faster the lower temperature of the corners .the reason is that the greater the thickness ratio of the slab, The larger the outer surface area and the air contact surface, the faster the heat dissipation.

G. S-S' Section PN Path Temperature Condition

Fig. 8a, Fig. 8b shows the heating stage temperature of the slab path PN, and Fig. 9a, Fig. 9.b shows the soaking temperature of the slab path PN. The same research method. The temperature distribution of the PN path of the two kinds of slabs is shown in Table V when $t_5 = 38.4s$.the two kinds of slab PN The path temperature distribution is shown when $t_6=110.64s$ in Table VI.

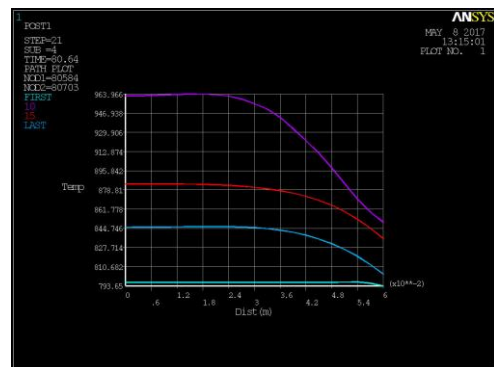


Figure 8.a t5= 38.4s, slab A

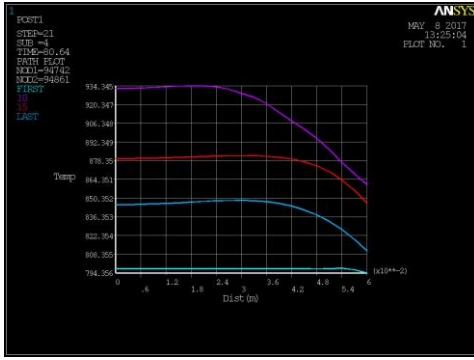


Figure 8.b t5 = 38.4s, slab B

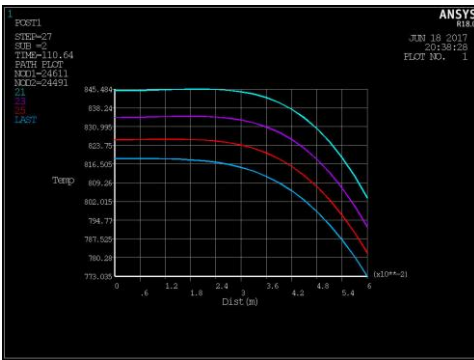


Figure 9.a t6 = 110.64s, slab A

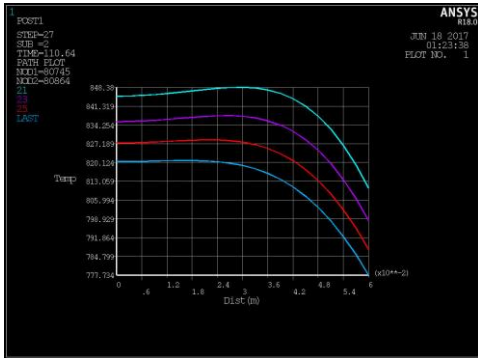


Figure 9.b t6 = 110.64s, slab B

TABLE V. T5 = 38.4S SLAB PATH PN TEMPERATURE COMPARISON

| Slabs | Side surface temperature | Corner temperature | Temperature difference |
|-------|--------------------------|--------------------|------------------------|
| A | 964.0 °C | 850.2 °C | 114.0 °C |
| B | 934.3 °C | 860.6 °C | 73.3 °C |

Analysis: In the induction heating of slab, t5 = 38.4s, the two slabs are the highest temperature in the central area of the side surface, the lowest temperature in the corner area. It is shown that the magnetic field in the central region of the side surface is the strongest in the induction heating process, the thermal effect of the eddy current is the strongest, the magnetic field in the corner region is the weakest, the eddy heat effect is the weakest and the temperature in the middle region is stable. with the greater the thickness ratio of the slab, the smaller the temperature fluctuation range on the PN path, the more uniform the temperature distribution.

TABLE VI. COMPARISON OF SLAB PATH PN TEMPERATURE IN SOAKING STAGE

| Slab s | Slab is hot before t5 = 80.64s | | | After slabs are hot, t6 = 110.64s | | |
|--------|--------------------------------|-------------|-------------------------------|-----------------------------------|-------------|-------------------------|
| | Side surface area | Corner area | Temperature fluctuation range | Side surface area | Corner area | Temperature fluctuation |
| A | 845.4 °C | 804.0 °C | 41.4 °C | 818.5 °C | 773.0 °C | 45.5 °C |
| B | 848.3 °C | 810.0 °C | 38.3 °C | 820.0 °C | 777.0 °C | 43 °C |

Analysis: The fluctuation range of PN path temperature is further expanded before and after the soaking of the two slabs, the wider the slab width and thickness ratio is, the smaller the temperature fluctuation range at the same time, the more uniform the temperature distribution on the PN path, The greater the maximum temperature in the central area of the side surface, the faster the lower temperature of the corner region is also declining. The reason is that the greater the thickness ratio of the slab, the greater the contact surface of the entire outer surface and the air, resulting in faster heat dissipation.

H. Effect of Insulation Cover on Slab soaking Process

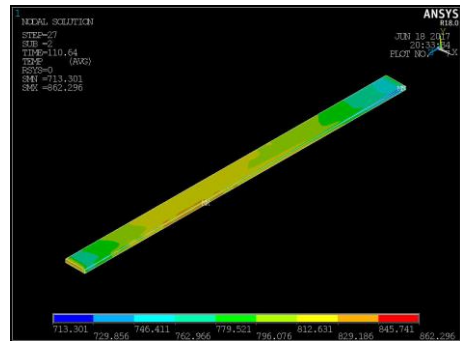


Figure 10.a Slab A, no insulation cover

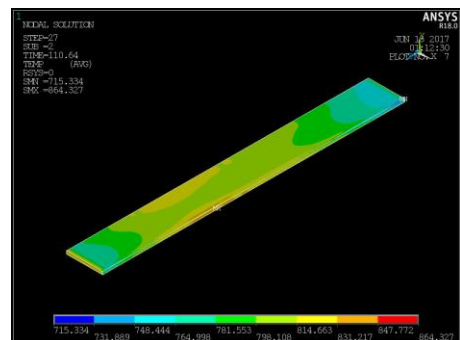


Figure 10.b Slab B, no insulation cover



Figure 11.a Slab A, with insulation cover

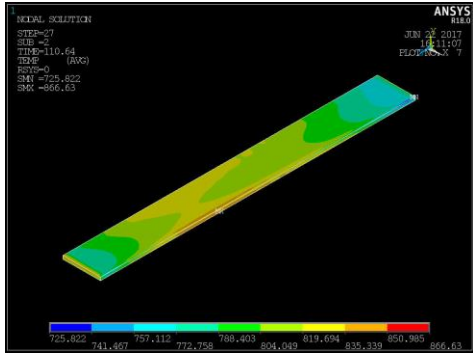


Figure 11.b Slab B, with insulation cover

TABLE VII. WITH OR WITHOUT INSULATION TEMPERATURE COMPARISON

| Slabs | No insulation cover | | Insulation cover | |
|-------|---------------------|--------------------|---------------------|--------------------|
| | Maximum temperature | Lowest temperature | Maximum temperature | Lowest temperature |
| A | 862.2 °C | 713.3 °C | 863.8 °C | 723.4 °C |
| B | 864.3 °C | 715.3 °C | 866.6 °C | 725.8 °C |

Analysis: Fig. 10a, Fig. 10b, Fig. 11a, Fig. 11b, with or without insulation masks when the temperature field contrast, as shown in Table VII, slab insulation cover when the maximum temperature and minimum temperature than the insulation when the high, so the soaking stage insulation cover When the temperature drop is lower than the non-insulation mask, insulation effect is obvious.

III. CONCLUSIONS

In this paper, ANSYS finite element method is used to simulate and analyze the temperature change of two kinds of slab induction heating and soaking. For the improvement of induction heating process of hot rolled slab, the following conclusions are drawn: 1) The greater the width to thickness ratio, the great temperature difference after induction heating. the corner part of the heat dissipation fast, low temperature, a reasonable heat for the corner part is needed in order to improve the temperature uniformity before rolling; 2)The reasonable setting of the socking periods help slab temperature tend to be uniform; 3)Adding insulation cover can effectively slow down the slab during soaking process. Of course, the slab induction heating process is faced with many challenges, such as the slab corner heat is still a problem, the follow-up need to focus on the slab corner part heat research. At the same time, the width to thickness ratio exceeds the normal range, and how to simulate induction heating on the ultra-thin slab is also a challenge. The induction heating process of hot rolled slab needs to be further improved.

ACKNOWLEDGMENT

Three-Dimensional Dynamic Finite Element Modeling and Simulation of Induction Belt Based on Kriging Interpolation.

REFERENCES

- [1] S. M. Fu, Z. Y. Wu, and S. Q. Cao, "Finite element method simulation of induction heating for a large marine crankshaft," *Advanced Materials Research*, 753-755:1035-1039, 2013.
- [2] P. Ali, K. Al, Shaikhli, *et al.*, "Study of power and field distributions in induction heating system by finite element method," *International Journal of Science and Engineering Research*, 2014.
- [3] K. H. Cho, "Coupled electro-magneto-thermal model for induction heating process of a moving billet," *International Journal of Thermal Sciences*, vol. 60, no. 1, pp. 195-204, 2012.
- [4] V. Demidovich and I. Rastvorova, "Precise induction heating of non-ferrous cylindrical billets," *Asian Journal of Applied Sciences*, 2014.
- [5] U. Ray, A. Sarkar, S. Sen, *et al.*, "Induction heating of an aluminum billet: A numerical study of the thermal behavior," *Applied Mechanics & Materials*, vol. 110-116, no. 1, pp. 58-76, 2012.
- [6] L. J. B. Qaseer, "Micro-T circuit model for the analysis of cylindrical induction heating systems," *IEEE Transactions on Energy Conversion*, vol. 25, no. 4, pp. 1021-1027, 2010.
- [7] Z. Xu, X. Che, B. He, *et al.*, "Model identification of the continuous casting billet induction heating process for hot rolling," in *Proc. Third International Conference on Intelligent System Design and Engineering Applications*, 2013, pp. 942-945.
- [8] Z. Xu, X. Che, B. He, *et al.*, "Research on temperature optimal control for the continuous casting billet in induction heating process based on ARX model," in *Proc. Chinese Intelligent Automation Conference*, 2013, pp. 777-786.
- [9] G. Xia and A. Schieffermüller, "The influence of support rollers of continuous casting machines on heat transfer and on stress-strain of slabs in secondary cooling," *Steel Research International*, vol. 81, no. 8, pp. 652-659, 2010.
- [10] M. Uotani, "Natural convection heat transfer in thermally stratified liquid metal," *Journal of Nuclear Science & Technology*, vol. 24, no. 6, pp. 442-451, 2012.



Cheng-Xiao Ming was born in Anhui Province, China, in 1992. Currently studying at the Automation College of Hangzhou DianZi University The direction of the study during the master is the slab induction heating modeling and simulation

Xu-Zhe, male, Zhejiang, professor, master guide, the main research areas are system modeling and optimization control, data mining, etc.

He-Bi-Shi Was born on October 21, 1981. Master of Computer Science.